

Extended Data Figure legends 1-10

Extended Data Figure 1. Characterization of expression patterns of EGFP-Shank3 and other synaptic proteins in *Shank3* transgenic mice. **a**, Description of the *Shank3* BAC used for TG mice generation (image was modified from UCSC genome browser). **b**, Western blot images show expression of EGFP-Shank3 in synaptic fraction of *Shank3* TG brain lysates. EGFP antibody recognized EGFP-Shank3 (~200 kDa) specifically in synaptic fractions of *Shank3* TG mice. Asterisk indicates non-specific bands detected by the EGFP antibody. Shank3 antibody detected endogenous Shank3 plus EGFP-Shank3 (arrow) in the TG samples. S2, soluble fraction; P2, crude synaptosomal fraction; PSD I, synaptic fraction after one time

Triton X-100 washout. **c**, The brain regional expression pattern of EGFP-Shank3 is similar to that of endogenous Shank3. Cb, cerebellum; Hp, hippocampus; St, striatum; Th, thalamus; Ct, cortex. **d**, The brain developmental expression pattern of EGFP-Shank3 is similar to that of endogenous Shank3. **e**, The fold changes of Shank3 proteins in 3-week-old TG mice (n=4) are similar to those of 6-week-old mice (Fig. 1d). **f**, Female TG mice (n=4) show similar fold changes of Shank3 proteins to male TG mice (Fig. 1d). **g,h**, Expression levels of excitatory (**g**) and inhibitory (**h**) synaptic proteins are not significantly altered, except Shank3, in the synaptosomal fraction of 8-week-old TG hippocampus and striatum (n=6). All data are presented as mean \pm s.e.m. *P* values ($*P<0.05$) were derived from unpaired, two-tailed Student's *t*-test.

Extended Data Figure 2. Behavioral characterization of *Shank3* transgenic mice. **a**, TG mice showed increased locomotor speed during the 30 min open-field assay. **b**, Female TG mice showed increased home-cage activity. **c**, TG mice have increased body weight compared to WT mice measured at 9 week (male WT: 28.1 ± 0.9 , male TG: 30.6 ± 0.7 , female WT: 20.1 ± 0.3 , female TG: 21.4 ± 0.4 , n=10-13; $*P<0.05$; unpaired two-tailed Student's *t*-test) and 15 week age (male WT: 32.4 ± 1.2 , male TG: 37.0 ± 1.3 , female WT: 23.6 ± 0.4 , female TG: 26.6 ± 0.9 , n=10-13; $*P<0.05$). **d**, Increased food intake by TG mice. Food intake was measured from single-caged female TG or WT mice from 6 to 10 week age. At 7 week (WT: 3.51 ± 0.05 , TG: 3.69 ± 0.06 , n=9-11; $*P<0.05$; unpaired two-tailed Student's *t*-test) and 9 week age (WT: 3.61 ± 0.07 , TG: 3.86 ± 0.05 , n=9-11; $*P<0.05$), food intake by TG mice was significantly higher than WT mice. **e,f**, In the 3-chamber assay, male (**e**) and female (**f**) TG mice did not show significant preference for novel mice to novel objects. **g**, TG mice spent significantly less time in close interaction with novel social partners. **h,i**, Stereotypy time (**h**) and activity count (**i**) during the 30 min open-field test were

normal in TG mice. **j**, Time spent in grooming during 10 min monitoring was normal in TG mice. **k**, Separation-induced ultrasonic vocalization was measured from WT and TG mice of postnatal day 6 to 13. TG mice made less calls than WT at postnatal day 13. **l**, At postnatal day 13, TG mice express more Shank3 proteins than WT mice. All data are presented as mean \pm s.e.m. * P <0.05, ** P <0.01, *** P <0.001. The summary of statistical analyses for behavioral assays is provided in Supplementary Table 1.

Extended Data Figure 3. Behavioral phenotypes of *Shank3* transgenic mice were rescued by crossing with *Shank3B*^{+/-} mice. **a**, Schematic diagram shows possible genotypic combinations and their Shank3 expression levels (arrow) from the crossing between *Shank3* TG mice and *Shank3B*^{+/-} mice. **b**, Quantification of the levels of Shank3 proteins in each genotype (n=4). The fold changes were compared to the WT (*Shank3B*^{+/+}) controls. Crossing of *Shank3* TG mice with *Shank3B*^{+/-} mice significantly decreased the levels of α isoform and total Shank3 protein. **c,d**, Locomotor activities of male (**c**) and female (**d**) *Shank3* TG mice were rescued by crossing with *Shank3B*^{+/-} mice. **e,f**, Immobile time in tail-suspension test of male (**e**) and female (**f**) *Shank3* TG mice were rescued by crossing with *Shank3B*^{+/-} mice. **g**, Prepulse inhibition (by 78 dB) of female *Shank3* TG mice was rescued by crossing with *Shank3B*^{+/-} mice. All data are presented as mean \pm s.e.m. * P <0.05; *** P <0.001.

Extended Data Figure 4. Basal synaptic transmission and NMDA receptor-dependent synaptic plasticity are normal at the hippocampal Schaffer collateral-CA1 synapses of *Shank3* transgenic mice. **a**, Images of cresylviolet staining show normal cytoarchitecture of TG brain. **b**, Normal paired-pulse facilitation ratio (PPR) of evoked EPSCs (eEPSCs) at TG Schaffer collateral-CA1 synapses. **c,d**, Normal synaptic input-output (I-O) relationship at TG Schaffer collateral-CA1 synapses. I-O curve (**c**) and cumulative curve of I-O slope (**d**) are

shown. Red lines in **c** represent the fitting curves. **e**, Left, sample traces of action potentials triggered by 200 pA current injection in hippocampal CA 1 region of WT and TG mice. Middle and right, unaltered number of action potentials triggered by the injection of current at different level (middle) and amplitude of the first action potential triggered by 800 ms-long pulse of 200 pA current (right) show normal intrinsic excitability of hippocampal CA1 pyramidal neurons in TG mice. **f**, Amplitude, frequency and decay of mEPSC are not altered in CA1 pyramidal neurons of TG mice. **g,h**, NMDA receptor-dependent long-term potentiation (**g**) and long-term depression (**h**) at Schaffer collateral-CA1 pyramidal synapses are normal in TG neurons.

Extended Data Figure 5. Generation and characterization of Shank3 *in vivo* interactome.

a, Isolation of EGFP-Shank3 protein and its interactors from synaptosomal fraction of TG mice. **b**, Venn diagrams show overlaps among the protein lists from Shank3 *in vivo* immunoprecipitation, Shank3 Y2H screening, and either published mouse PSP (postsynaptic proteome) or human PSD. **c**, Shank3 interactome network. **d**, Average path length of Shank3 interactome (3.12, red line) is significantly ($P < 0.0001$) shorter than that of mouse PSP interactome (mean=3.91, black line), supporting strong connectivity of Shank3 interactome. **e**, GO and KEGG pathway analysis of Shank3 interactome reveal enrichment of actin cytoskeleton-related function/pathway. The full result of analysis is in Supplementary Table 5. **f**, Confirmation of the *in vivo* interactions between Shank3 and actin-related proteins. **g**, In cultured hippocampal neurons, ARPC2 proteins are co-localized with F-actin (upper panel) and EGFP-Shank3 (lower panel).

Extended Data Figure 6. Shank3 siRNA reversed increased F-actin levels and ARPC2 cluster size in cultured hippocampal pyramidal neurons from Shank3 transgenic mice. a,

Validation of the two siRNAs against *Shank3*. HEK293T cells were transfected with HA-Shank3 plus control or *Shank3* siRNA. EGFP plasmid was co-transfected as an internal control. After 48 hr, expression levels of HA-Shank3 were measured by western blot and quantified (n=3). **b**, si-*Shank3* reversed the increased F-actin levels of *Shank3* TG neurons. Image for si-*Shank3* #2 is not shown. **c**, si-*Shank3* reversed the increased ARPC2 cluster size of *Shank3* TG neurons. All data are presented as mean \pm s.e.m. from 20-30 neurons per condition. *P* values ($*P<0.05$, $**P<0.01$) were derived from one-way ANOVA with post hoc Tukey's multiple comparison.

Extended Data Figure 7. Normal excitatory and inhibitory synapse numbers of GAD-6-positive inhibitory neurons of *Shank3* transgenic mice. **a**, Expression of EGFP-Shank3 in GAD-6-positive inhibitory neurons of *Shank3* TG mice. The yellow circles of dotted line and solid line indicate neuronal cell bodies of a GAD-6-negative excitatory neuron and a GAD-6-positive inhibitory neuron, respectively. The box 1 shows dendritic segment of the excitatory neuron and the box 2 shows that of the inhibitory neuron. **b**, Quantification of dendritic EGFP-Shank3 intensity in excitatory and inhibitory TG neurons. Inhibitory neurons express less EGFP-Shank3 (excitatory neurons: 1.00 ± 0.06 , inhibitory neurons: 0.74 ± 0.09 , n=10; $*P<0.05$; unpaired two-tailed Student's t-test). **c**, Normal excitatory synapse number of GAD-6-positive inhibitory neurons of *Shank3* TG mice. **d**, Normal inhibitory synapse number of GAD-6-positive inhibitory neurons of *Shank3* TG mice. **e**, Quantification of (c) (WT: 1.00 ± 0.10 , TG: 0.99 ± 0.07 , n=18; $P>0.05$; unpaired two-tailed Student's t-test) and (d) (WT: 1.00 ± 0.12 , TG: 0.95 ± 0.09 , n=20; $P>0.05$; unpaired two-tailed Student's t-test).

Extended Data Figure 8. Shank3 interactome is connected with Gephyrin-interacting actin-related proteins, Mena, Profilin1 and Profilin2. Based on literature search, we

selected candidate actin-related proteins (Mena/VASP, Profilin1 and Profilin2) that directly interact with inhibitory postsynaptic protein Gephyrin. To understand potential interactions among these proteins and the Shank3 interactome, we generated interaction network using the information from our Y2H screening and IRefIndex PPI database (<http://irefindex.uio.no/wiki/iRefIndex>). The interaction network shows that Mena/VASP, Profilin1 and Profilin2 are connected with Shank3 interactome mainly through actin-related proteins. Note that one of the Gephyrin-interacting proteins, Profilin2, was also identified by our Shank3 *in vivo* IP (Supplementary Table 4).

Extended Data Figure 9. Mania-like behaviors of *Shank3* transgenic mice are resistant to lithium treatment. **a**, Basal and amphetamine-induced locomotor activities of female TG mice were not affected by lithium treatment. **b-e**, Abnormal acoustic startle response (**b,d**) and PPI (**c,e**) of male and female TG mice were not rescued by lithium treatment. **f,g**, Immobile time of male (**f**) and female (**g**) TG mice in tail-suspension test was not rescued by lithium treatment. WT female mice showed decreased immobile time upon lithium treatment, which is an expected response to high dose lithium treatment in WT mice. All data are presented as mean \pm s.e.m. * $P < 0.05$; *** $P < 0.001$.

Extended Data Figure 10. Valproate treatment does not affect synaptic protein and F-actin levels in neurons of *Shank3* transgenic mice. **a**, One hr after final valproate injection (200 mg/kg), synaptosomal fraction was prepared from brains, and indicated proteins were detected by western blotting. Neither WT nor TG mice showed significant change in the levels of synaptic proteins by valproate treatment (n=7). **b**, Representative confocal images of *Shank3* TG cultured hippocampal pyramidal neurons (DIV 14) treated with different concentrations of valproate (0, 0.01, 0.1 and 1 mM) for 30 or 60 min. **c**, Quantification of (**b**).

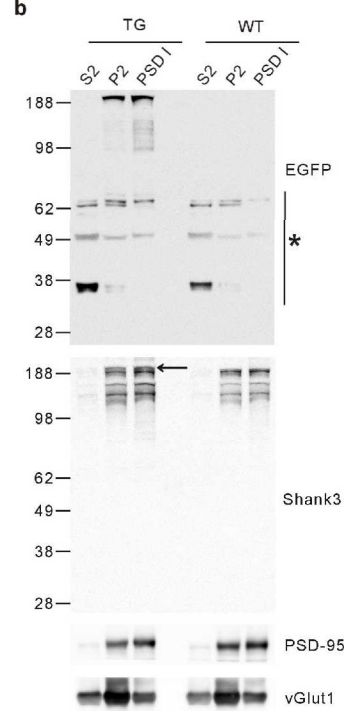
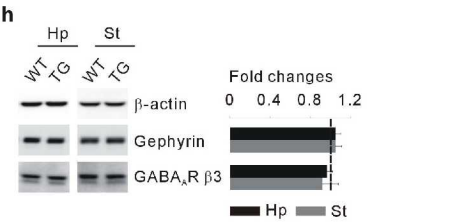
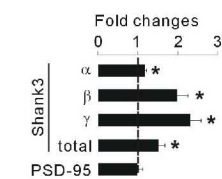
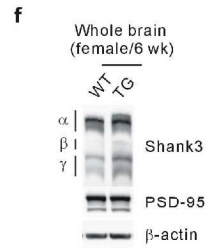
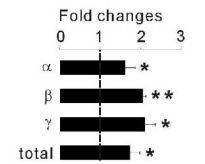
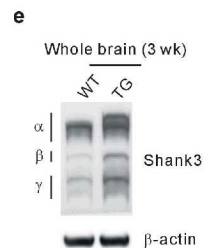
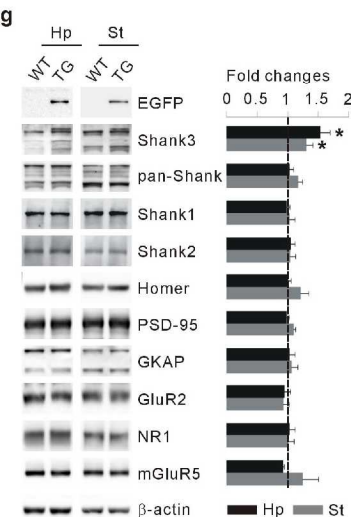
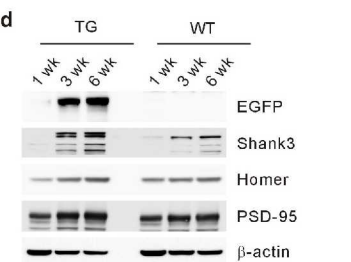
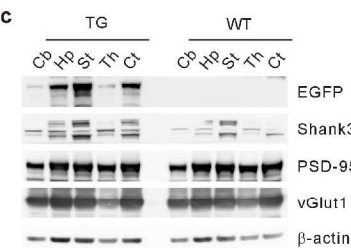
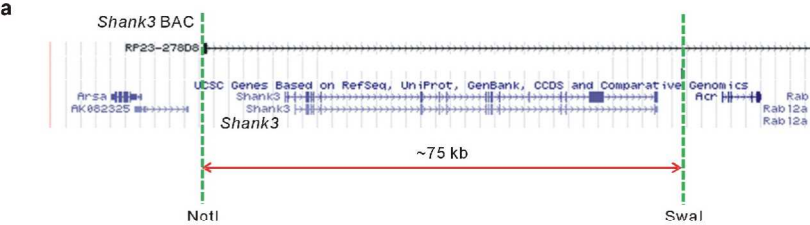
There was no significant change in F-actin levels by valproate treatment (n=16 per condition).

All data are presented as mean \pm s.e.m.

Type of file: figure

Label: 7

Filename: figure_7.jpg

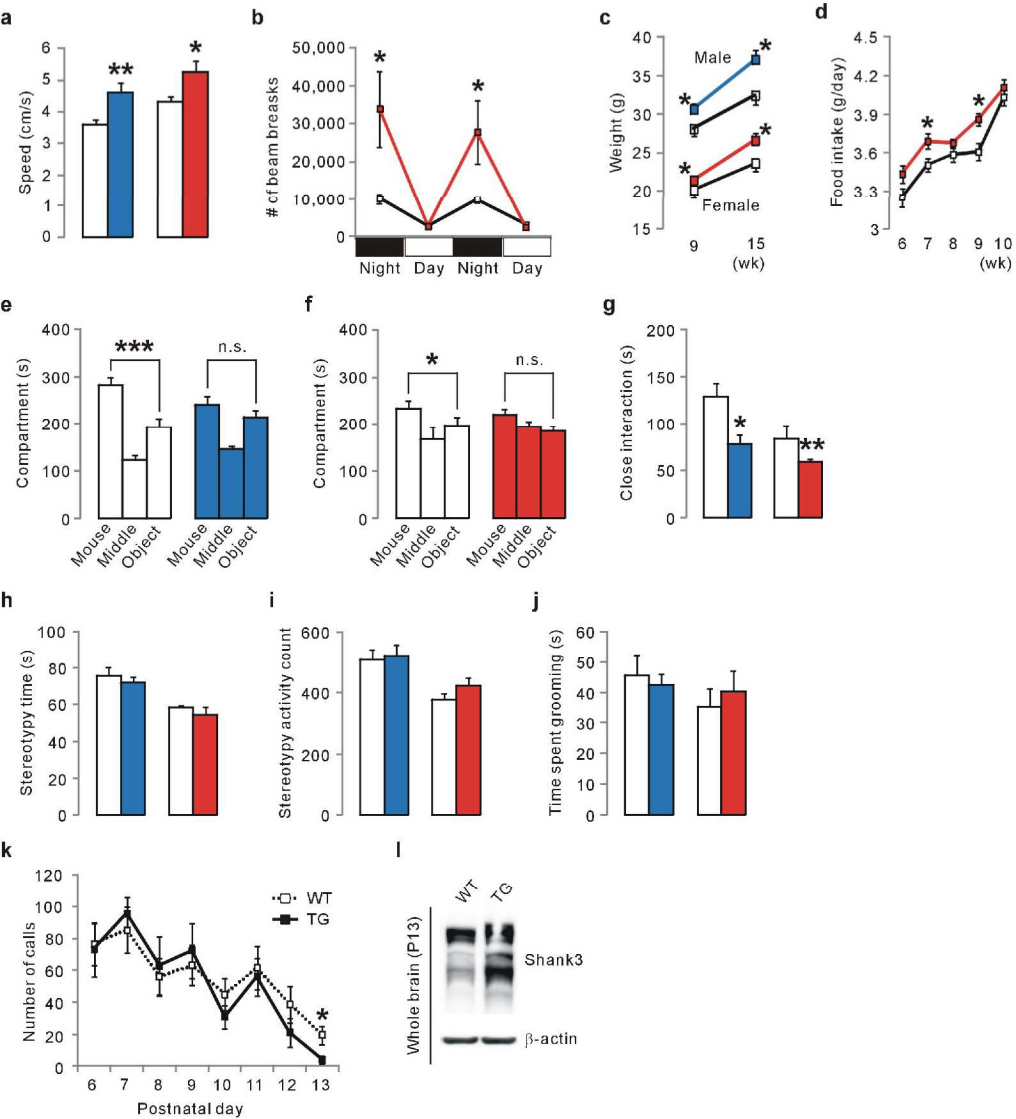


Type of file: figure

Label: 8

Filename: figure_8.jpg

WT TG male TG female



Type of file: figure

Label: 9

Filename: figure_9.jpg

a*Shank3*^{TG} X *Shank3B*^{+/-}

Offspring

TG / *Shank3B*^{+/+} ↑

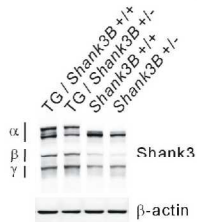
TG / *Shank3B*^{+/-} ●

Shank3B^{+/+} ●

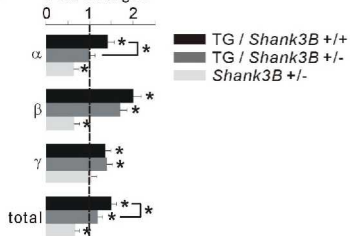
Shank3B^{+/-} ↓

b

Whole brain (10 wk)

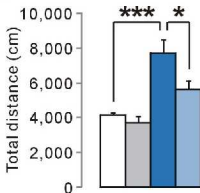
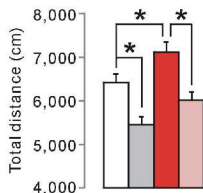
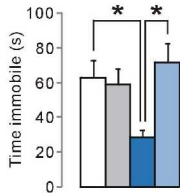
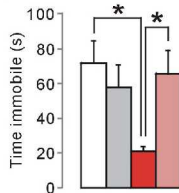
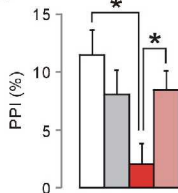


Fold changes



□ WT ■ TG male ■ TG female

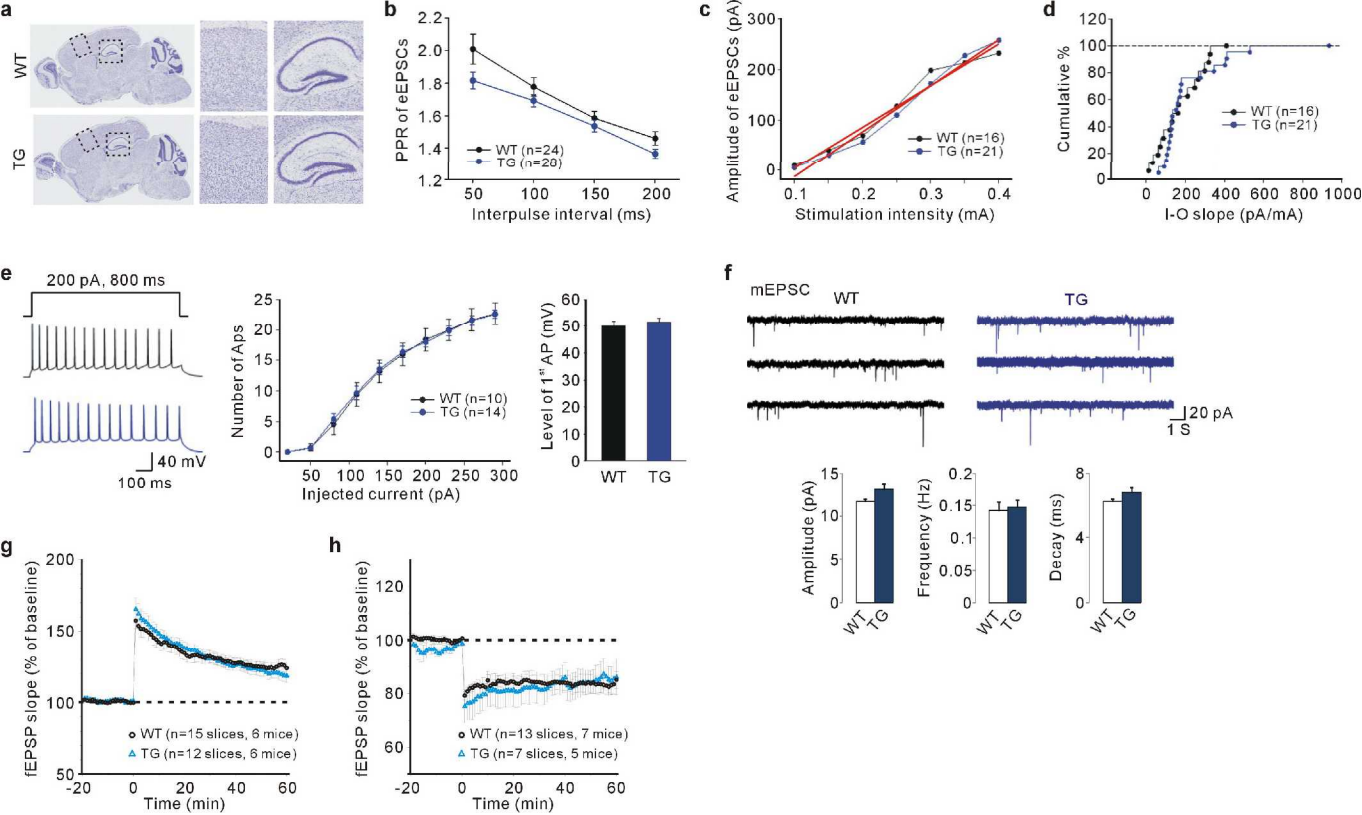
■ *Shank3B*^{+/-} ■ TG / *Shank3B*^{+/-} male ■ TG / *Shank3B*^{+/-} female

c**d****e****f****g**

Type of file: figure

Label: 10

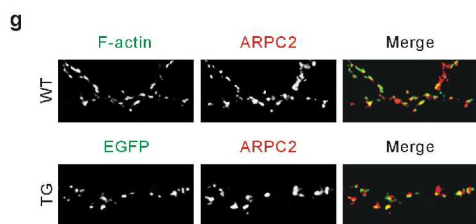
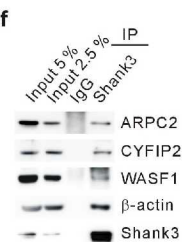
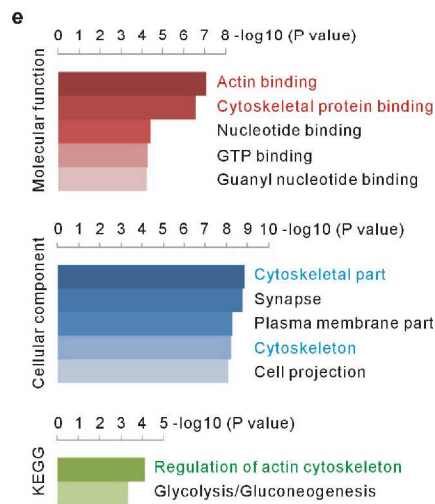
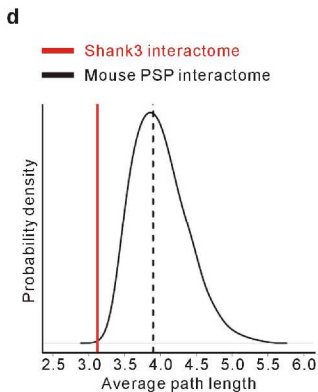
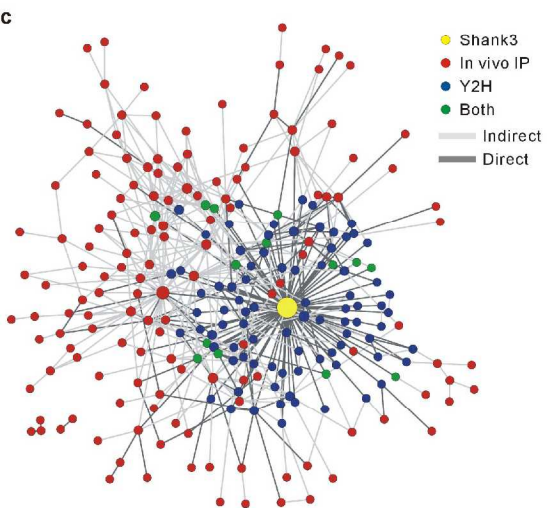
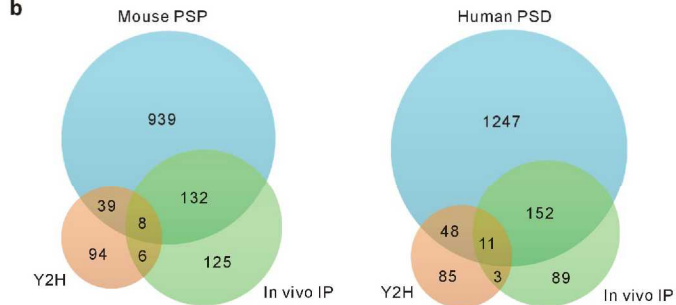
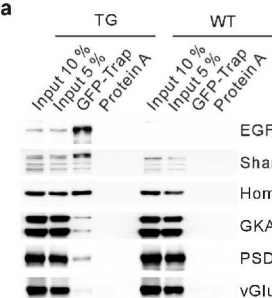
Filename: figure_10.jpg



Type of file: figure

Label: 11

Filename: figure_11.jpg



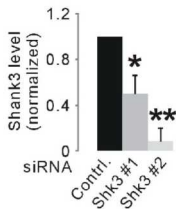
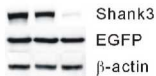
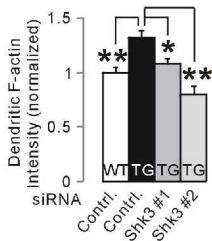
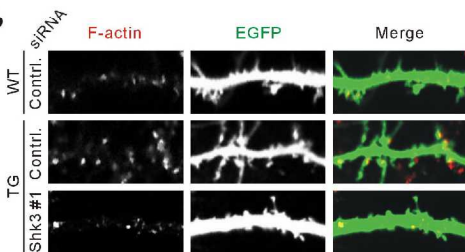
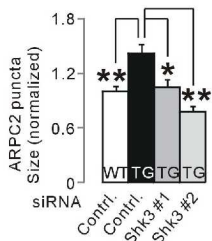
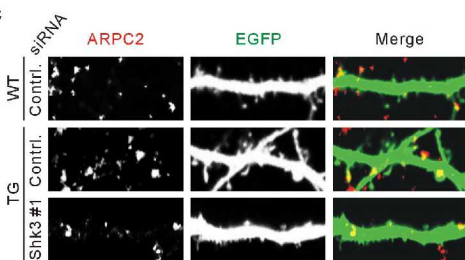
Type of file: figure

Label: 12

Filename: figure_12.jpg

a

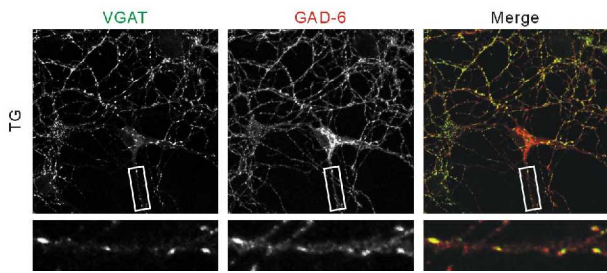
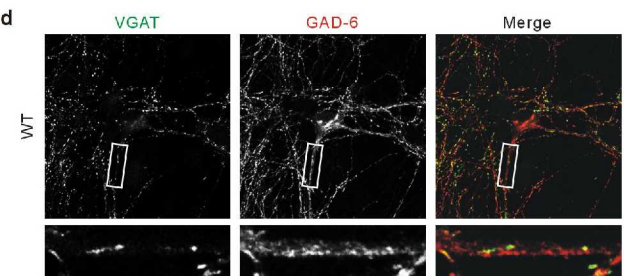
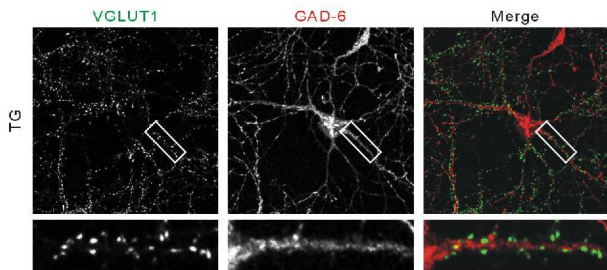
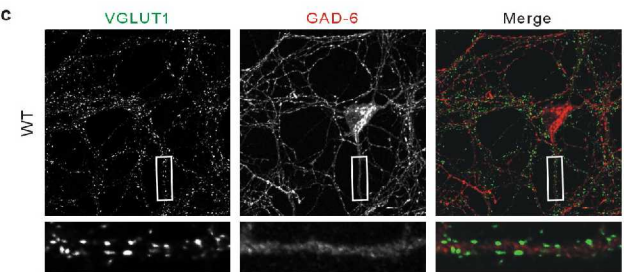
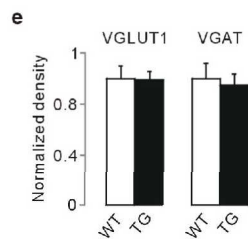
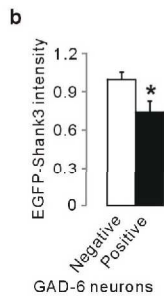
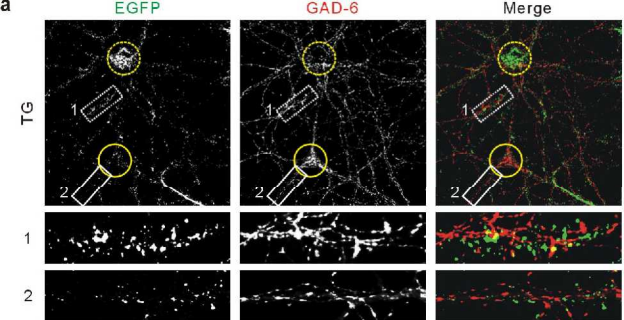
| | | | |
|--------------|---|---|---|
| HA-Shank3 | + | + | + |
| EGFP | + | + | + |
| si-Control | + | | |
| si-Shank3 #1 | | + | |
| si-Shank3 #2 | | | + |

**b****c**

Type of file: figure

Label: 13

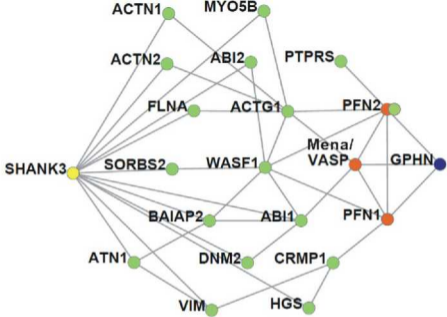
Filename: figure_13.jpg



Type of file: figure

Label: 14

Filename: figure_14.jpg



● Shank3

● Shank3 interactome

● Actin-related interactors of Gephyrin

● Gephyrin

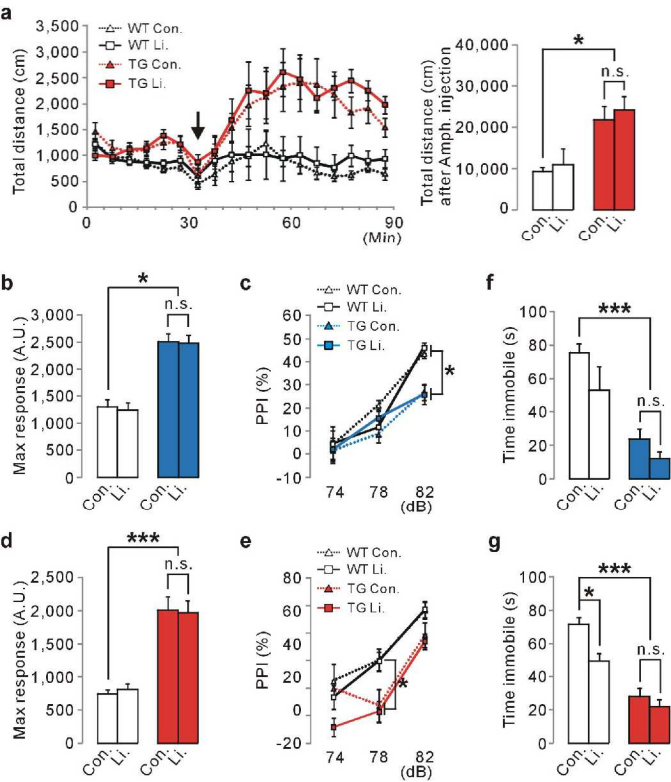
— Direct interaction

Type of file: figure

Label: 15

Filename: figure_15.jpg

WT TG male TG female



Type of file: figure

Label: 16

Filename: figure_16.jpg

